AADE-19-NTCE-086

A Novel Approach to Investigate Cement Pore Pressure during Hardening

Weicheng Zhang, Steven Hilgedick and Andreas Eckert, Missouri University of Science and Technology

Abstract

Cement sheath integrity is key to wellbore zonal isolation and preventing fluid migration along the wellbore. Different types of failure, including debonding (micro-annuli), radial cracking, and shear failure, can occur as a result of downhole conditions throughout the life of the well. The initial state of stress is the basis for failure prediction, however previous methods to estimate or measure cement pore pressure are based on samples cured at surface conditions and/or in the absence of surrounding formation water. This paper presents a novel approach to cement testing, combined with numerical modeling, to better understand and characterize cement hardening and corresponding fluid pressure changes during hardening. The laboratory setup is designed to measure the evolution of cement fluid pressure throughout cement hardening under in-situ conditions, including the presence of formation water. During the curing process, a fluid pressure sensor is embedded within Class G Portland cement within a vessel maintaining constant pressure while immersing the specimen in water, thus allowing water to enter the sample throughout the process. The final cement pore pressure is used in the initial state of stress within the cement sheath for numerical modeling and failure analysis during subsequent operations and well conditions. Numerical models are shown comparing established laboratory results to common assumptions for the initial pore pressure and state of stress in the cement sheath. A better understanding of cement hardening under in-situ conditions has the potential to improve wellbore integrity prediction, and well design, lowering costs related to wellbore failure issues.

Introduction

In the oil industry, cement is the key component of the wellbore system. During the cementing operation, cement slurry is injected into the annulus between two casings or casing and formation. The liquid cement slurry then gradually hardens and transforms into a solid matrix. The impermeable cement sheath provides casing strings with mechanical support and isolates different zones to prevent unwanted formation fluid migration along the wellbore. Failure of the cement sheath can significantly compromise wellbore integrity and induce severe consequences including reduction in the injection/production efficiency, contamination of the freshwater aquifer, acceleration of the casing erosion, etc.

Cement hardening process

To prevent cement failure and ensure wellbore integrity throughout the entire wellbore life cycle, it is critical to understand the behavior of the cement sheath during the hardening process. Cement hardening is a complicated hydration reaction that involves chemical, thermal, and mechanical processes. During the hardening process, the cement paste gradually consumes water, develops the porous skeleton, gains strength, adheres with the casing and the formation rock, and becomes an impermeable barrier (Nelson and Guillot, 2004). The cement hydration reaction is highly affected by external conditions. Factors such as water supply, curing temperature, and curing pressure can directly affect the hydration rate, cement volume variation, and mechanical property development of the cement (Nelson and Guillot, 2004). Therefore, replicating downhole conditions where the cement hardening takes place is necessary to understand the behavior of the cement paste during hardening and to further evaluate the influence on cement failure. It needs to be noted that the cement hydration reaction is a long-term process and can last for months (Nelson and Guillot, 2004). It needs to be clarified that the cement hardening process investigated in this paper mainly refers to the WOC period which may last 24 to 48 hours.

State of stress and pore pressure evolution during cement hardening

The in-situ wellbore state of stress is the critical parameter that directly determines the occurrence, type, and the damage severity of failure in the cement sheath. When the cement paste is pumped into the annulus, the liquid cement paste features an isotropic state of stress, which is equal to the cement slurry pressure. During the hardening process, the water content in the cement paste is consumed and the solid skeleton is developed. The solid skeleton starts to develop the pore space and further isolates this pore space. The migration of water in the cement matrix and the fluid communication between the cement and formation become more difficult. Hence, the cement permeability begins to decrease, and the fluid pressure in the pore space may start to drop below the initial cement slurry pressure (Appleby and Wilson, 1996). Bois et al. (2011) proposed that the fluid trapped in the isolated pores within the cement matrix may be entirely or partially consumed by further hydration reactions, and the pore pressure in the cement may continue to decrease even below the formation pressure. Depending on the sufficiency of water supply from the formation and the pressure in the annulus, a certain amount of water may flow into the cement matrix to compensate the water consumed by the hydration reaction during the period that the cement matrix is still permeable. Thus, the pore pressure in the cement can be maintained at the pore pressure of the formation. Therefore, the intrinsic properties of the formation, such as water saturation and permeability, should also affect cement hardening under downhole conditions and the resulting cement state of stress at the end of hardening.

In the past various assumptions have been made with respect to the state of stress and pore pressure in the set cement as the initial conditions for subsequent failure analysis. Ravi et al. (2002) assumed two end-member scenarios for the cement state of stress: either the cement sheath has a hydrostatic pore pressure and an isotropic state of stress equal to cement slurry pressure minus pore pressure; or the cement sheath has a hydrostatic pore pressure and zero effective stress. Based on numerical simulation results, Boukhelifa et al. (2004), Nygaard et al. (2012), and Zhang et al. (2017) proposed that the set cement should have a compressional state of stress otherwise failure may occur easily. Zhang and Eckert (2018) investigated the potential pore pressure decrease during cement hardening and found the pore pressure drop has different influences on different interfaces (casing-cement or cement-formation). Lab measurements of cement pore pressure evolution during the hardening process were also conducted. Levine et al. (1979) measured the fluid pressure at the top and bottom of a 12ft-long annulus which is filled with cement slurry and a 38ft-long water column was connected to the top of the cement body provided the confining pressure. The pressure at the bottom of the cement column dropped from 24 psi to 4 psi in 4 hours. Appleby and Wilson (1996) studied the permeability variation during the cement hardening process. They measured the fluid pressure at one side of a pressurized cylinder chamber while the other side is connected to the external water source. They found that the cement pore pressure drops drastically (50% by the end of measurement), if no external water is supplied and cement pore pressure drops slightly (5%) with abundant water supply. Reddy et al. (2009) provided the measurement of cement pore pressure during hardening together with the measurement of cement shrinkage. They found that the cement shrinkage rate can be correlated to the pore pressure decrease during different periods of the hardening process.

It should be noted that the outer boundary of the cement placed in the annulus between the casing and formation is in direct contact with the formation. For permeable formations, there may be sufficient contact area that allows the formation water to easily enter the cement sheath when the impermeable cement matrix has not been established. For the test carried out on a cylindrical cement sample with pressure supplied to one end and measured on the other, insufficient exposure to formation water may not represent the pore pressure in the entire cement body.

In this study, we introduce a novel measurement set-up to cure the cement slurry under pressurized conditions with water surrounding the curing sample, while measuring the cement pore pressure in the center of the sample. Measured cement pore pressure during its transitional phase from a fluid to an impermeable porous media provides insight into and indicates the need for further study to investigate the state of stress evolution during cement hardening.

Experimental set-up

The novel experimental set-up presented in this work is designed to cure the cement paste under a high confining pressure (1500psi). The high temperature that represents the formation temperature has not been included in the design of this set-up. It is primarily designed to investigate the influence of high curing pressure and the thermal control unit may be incorporated into this set-up for future testing.

Fig. 1 shows a diagram of the experimental set-up which includes a pressure vessel, cement mold within the vessel, fluid pressure sensor, and the pump to control the pressure. The pressure vessel consists of the top and end caps, a chamber of 7 in diameter with high strength steel rods sealing the top and bottom caps to the cylinder, and two ports supplying pump pressure and allowing the cylinder to be filled with water and pressure to be released from the cell. The mold includes the stainless steel mesh and fiberglass membrane to hold the cement slurry in place and allow the surrounding water to enter the curing cement. The fluid pressure sensor is contained within an impermeable membrane to prevent the cement invasion into the sensor body. Water is contained within the membrane and sensor body, and all air bubbles were eliminated. The data acquisition system provides power to and measures the response from the sensor. The membrane protected sensor and data acquisition system were calibrated to ensure the accuracy of the measurement. Two bench tests were performed for calibration: one test included submerging the sensor in a 10ft concrete column, and one where water at the top of the cement column was pressurized to 2000psi.

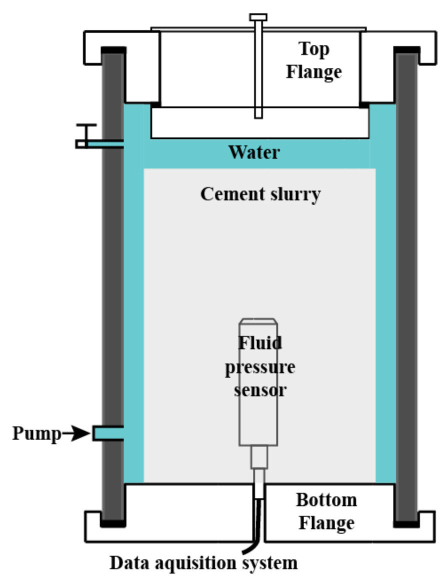

Fig. 2. Diagram of experimental set-up for measuring cement pore pressure evolution during hardening

Test preparation and initiation

Neat Portland Class G cement was used in this study. The water cement ratio (w/c) chosen was 0.44, which corresponds with the API recommendation (API 10A). The mixing procedure followed API standards. The cement paste was injected to the pressure vessel at a low injection rate and no visible air bubble were observed in the paste.

The top flange was installed and the rods were tightened. Confining pressure on the cement paste was increased to 1400psi throughout 30 minutes. The test was performed under room temperatures.

Results

Fig. 2 shows the cement pore pressure recorded during the 39 hours of testing time. Fig. 2 includes the pressure increase with a constant pumping rate of 10 mL/min during the 30 minutes of pressurization, as well as pressure stabilization period and the pore pressure decline recorded during the curing process. Throughout the curing process, the pump providing confining pressure to the water surrounding the cement paste was monitored and remained stable for 38 hours.

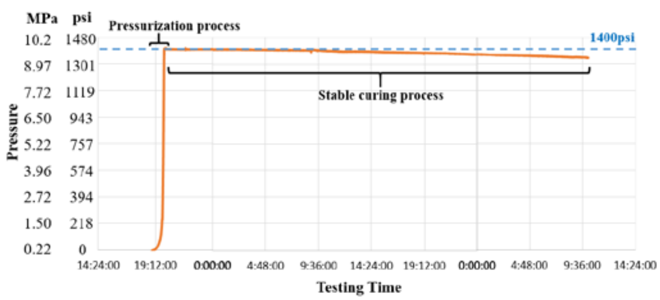

Fig. 2. Cement pore pressure data recorded during the test.

In order to better visualize the cement pore pressure drop during cement hardening, the stable curing process is displayed with a narrowed pressure range in Fig. 3. During the first 6 hours of the hardening process, (section A to B in Fig. 3), the cement pore pressure remains nearly equal to the confining pressure applied. After this, the cement pore pressure begins to drop from 1400 psi (point B) to 1339 psi (point E) with a gradually increasing rate. Point C and D indicate short pressure drops that occurred as the pump was being refilled over a 1-minute interval. The cement pore pressure dropped 14 psi at point C and 1.5 psi at point D. It needs to be mentioned that during the entire stable curing process, no leakage was observed and a total of 2.7oz (80ml) of water was pumped into the vessel.

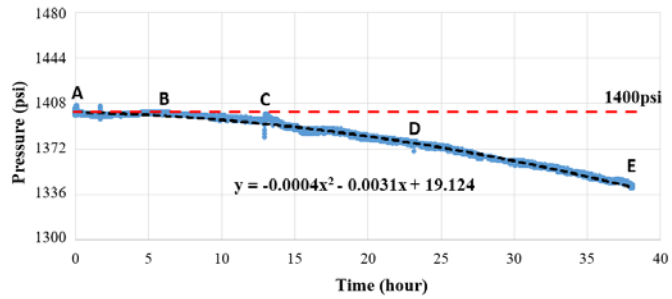

Fig. 3. Detailed examination of the stable curing process. The time is labelled as the time after the pressure vessel was stabilized at 1400psi.

Discussion

In this chapter, the measurement results are analyzed and compared with other experimental and numerical studies. The development of cement state of stress and the corresponding influence will be discussed.

Cement pore pressure variation

Fig. 3 shows that the pore pressure measured from the center of the cement sample dropped 4.4% (61 psi out of 1400 psi) during 38.5 hours. Appleby and Wilson (1996) reported a cement pore pressure dropped of 5% (0.1 MPa out of 2 MPa) in 10.2 hours if the cement sample is accessible to external water, and 49% (0.98 MPa out of 2 MPa) if not accessible. The general cement pore pressure decline tendency between this study is very similar to Appleby and Wilson (1996). The cement sample maintains the pore pressure equal to the confining pressure for 6.5 hours in this study (section A to B in Fig. 3), which is close to the 7-hour duration in the study by Appleby and Wilson (1996). The pore pressure decline in this study shows a gradual initial rate of increase (section B to C in Fig. 3) and appears nearly linear for the remainder of the test (section D to E in Fig. 3), which is also in agreement with Appleby and Wilson (1996). In the first 6 hours pressure maintenance is about equal, but our study loses pressure from 6.5 to 38 hours while theirs from 7 to 10. A detailed examination of the pore pressure decline and correlation with permeability measurements from similar studies is included later in the discussion.

The difference between the two measurement set-ups can be the primary reason to explain the slower and slightly lower cement pore pressure decline observed in this study. In the study of Appleby and Wilson (1996), the cement is only in contact with water at one end of the cylinder containing the sample, while in this study the cement sample is surrounded by water (aside from the bottom). Though the amount of external water consumption was not recorded or reported by Appleby and Wilson (1996), the amount of contact area to the external aquifer may affect the volume of water imbibition into the cement during hardening from the surrounding environment. Multiple studies (Appleby and Wilson, 1996; Backe et al. 1999; Bios et al., 2012; Lavrov and Torsæter, 2016) have confirmed that the amount of water supplied by the formation can directly and significantly affect the pore pressure magnitude in the cement.

Other factors may explain observed differences in results between these two studies. High curing pressure of the cement may accelerate the hydration reaction (Pang et al. 2013). The accelerated cement hydration reaction may lead to more rapid development of the impermeable cement matrix. The earlier the cement becomes less permeable, the easier the pressure difference between the cement pore pressure and the formation pressure is maintained, and as a result the cement pore pressure will drop at a faster rate (Appleby and Wilson, 1996; Backe et al. 1999, Nelson and Guillot, 2004). This study shows cement pore pressure began to drop slightly earlier, which indicates the hydration rate of this study is slightly higher. Hence, for tests that are conducted in room temperature (i.e. Appleby and Wilson, 1996 and this study), the cement hydration reaction is largely affected by the abundancy of water supply.

In addition, though the analysis of this study is based on the assumption that the cement is an isotropic medium, the potential influence of the distance from the sensor to supplemental water may also have a minor influence to the pore pressure profile, which may be a function of distance from the formation.

Cement state of stress evolution, cement pore pressure variation, and cement failure occurrence

As mentioned previously, the development of the cement state of stress during the hardening process is the key parameter for further wellbore integrity evaluation. However, due to the difficulty and limitation of downhole measurements, the cement state of stress can only be indirectly obtained from other measurements and indicators (i.e. leak-off test, cement bond log) in field operations. Laboratory experiments greatly supplement the knowledge gap by providing the variation of several parameters that are mechanically associated with the cement state of stress evolution (Justnes et al. 1995; Appleby and Wilson, 1996; Backe et al. 1999; Reddy et al. 2009). These parameters include the cement volumetric shrinkage (bulk/autogenous shrinkage), cement permeability variation, cement elastic property development, and cement pore pressure variation (Bois et al. 2012). In order to better understand the evolution of the cement state of stress and its influence on the resulting wellbore integrity, the cement pore pressure data of this study was combined with the rest of these parameters and analyzed with respect to the cement state of stress. It needs to be noted that the testing condition, cement type, and measurement method may vary in different studies. This section primarily focuses on the general variation tendency of each parameter and provides qualitative analysis of their temporal evolution and corresponding influences to the cement state of stress. The general temperature vs. time profile for the cement hydration process (Fig. 4) is used to assist in the illustration and analysis.

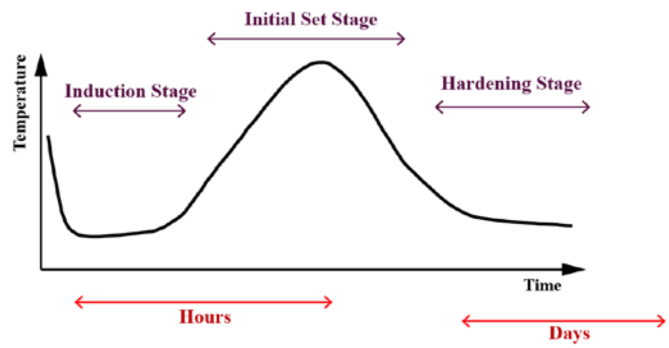

Fig. 4. The general temperature vs. time profile for the cement hydration process. The figure is adapted from Appleby and Wilson (1996) and Nelson and Guillot (2004)

Cement shrinkage during hardening is the most important factor affecting the state of stress evolution. The cement volume reduction is associated with the hydration reaction because the cement paste occupies more space than the developed solid porous matrix. Bulk or autogenous shrinkage refers to this reduction of cement volume during hydration. Wellbore integrity can be compromised by cement shrinkage majorly in two ways. Excessive shrinkage during hardening can directly create a gap (debonding failure) at the cement-casing and the cement-formation rock interfaces. Even if the shrinkage is not enough to initiate debonding failure, the tensile stress induced by the shrinkage can also make the interfaces and cement matrix more susceptible to debonding failure and radial cracking with subsequent wellbore operations further increasing tensile stress concentrations and failures (i.e. borehole pressure drop, injection of low temperature fluids; Bois et al. 2014). During the various stages of the cement hardening process the amount of shrinkage is not uniform. As a result, the influence on the cement state of stress is changing. Thus, the cement shrinkage must be correlated to the variations of other parameters (such as elastic properties, pore pressure, temperature, and strength) based on their interaction during the different stages.

Permeability is directly related to the development of the solid skeleton during the cement hardening, and it is the determining factor for the pore pressure variation in the cement. Backe et al. (1999) measured the cement permeability with gas flowing through a pressure cell and found that the permeability decreases from 90 mD at 3.5 hours to 20 mD at 6 hours (class G cement with retarder at 90°C). Permeability measurements using the U-Shaped permeameter and shrinkage test cell by Appleby and Wilson (1996) showed that from 7.1 hours to 15.7 hours of cement hardening, the permeability drops from 0.2 mD to 2×10^{-5} mD. The initiation of the permeability decrease falls in the curing time range of the Induction Stage and the drastic permeability decrease occurs in the Initial Set Stage (Fig. 4). As mentioned previously, the pore pressure measurement of this study started to drop after 6.5 hours of curing (point B in Fig. 3). The permeability of the cement sample at this time should be in the range of 1-0.1 mD, which can be viewed as a permeable matrix. Cement pore pressure then dropped 4.5 psi from point B to C within 7 hours (0.643 psi/hour), further decreased 18 psi from point C to D within 10 hours (1.8 psi/hour), and declined 36 psi from point D to E within 15 hours (2.432 psi/hour).

The period A to B (0-6.5 hours) illustrates the Induction Stage. During this stage, the cement is highly permeable, porosity is high, cement can easily flow, cement shrinkage is prominent, and cement may feature a visco-elastic behavior (Bois et al. 2014; Lavrov and Torsæter, 2016). However, the shrinkage may only have a minor influence on the state of stress in the cement due to the low stiffness and the relaxation tendency of the visco-elastic cement (Eckert and Zhang, 2015). The cement column can essentially flow to compensate for pore volume reduction.

The transition should occur from time A to time B, and time B to time D (6.5-23.5 hours) should belong to the range of the Initial Set Stage. During the Initial Set stage, the cement becomes unable to flow and the permeability decreases drastically and is comparable to the permeability range of impermeable rocks (Wang, 2000). As cement behaves more like an elastic material it quickly gains strength (Backe et al. 1999; Zhang et al. 2010). Under downhole conditions, the shrinkage primarily affects stresses in the radial and hoop directions of the cement sheath and induces higher stress variations (Lavrov and Torsæter, 2016).

The time period from time D to time E (24-35.5 hours) represents the pore pressure evolution during the cement Hardening Stage. The permeability of the cement continues to decrease and the cement becomes completely impermeable. The matrix is then unable to draw water from the surroundings. Based on poroelasticity theory (Wang, 2000), the significant decrease of cement pore pressure can greatly contribute to the cement shrinkage occurring during this stage, even becoming the predominant driving force for the shrinkage ((Nelson and Guillot, 2004; Bois et al. 2012; Lavrov and Torsæter, 2016). During this stage, the cement sheath behaves predominantly elastically and the amount of shrinkage that occurs during this stage has a more direct and critical influence on the state of stress in the cement, which greatly adds tensile stresses to the cement sheath (Nelson and Guillot, 2004; Lavrov and Torsæter, 2016). As a result, the risk of debonding failure occurrence at the casing-cement and cement-formation interfaces may be increased (Bois et al. 2012; Zhang and Eckert, 2018)

Insights for further studies

The major improvement of this experimental set-up compared to previously available testing procedures is the increased contact area and the constant availability of water to the cement during curing, which better represents the actual curing conditions. Measurement results shows that the increased contact area slows down the pore pressure reduction in the cement. Hence, further experimental studies can be carried out to include the effect of the distance of the sensor from the water cement interface. Detailed quantification of water supply abundancy (i.e. pore pressure borehole pressure differences, permeability) and resulting cement pore pressure profile can also be further investigated. This work could also include a thorough investigation of the effect of variation in curing conditions and formation rock properties (Lavrov and Torsæter, 2016; Zhang and Eckert, 2018).

Reflections from the result of this study can also greatly benefit numerical modeling studies. Rather than implementing an assumption based fixed pore pressure magnitude in numerical models (Gray et al. 2009, Nygaard et al. 2014; Zhang and Eckert, 2018), the evolution of pore pressure can be used as a critical input parameter as the pore pressure directly influences the effective stet of stress in the cement. The measurement result shows that the pore pressure decrease occurs more rapidly during the Initial Set and Hardening Stages, during which the cement can be viewed as an elastic matrix. The mechanical influence of the pore pressure drop and shrinkage should have the most significant influence to the state of stress in the cement and should be specially emphasized and simulated by numerical modeling studies.

Summary and outlook

This study has presented a new measurement approach of cement pore pressure during cement hardening under downhole conditions. From the measurement result and further analysis, several conclusions can be made:

.

- The experimental set-ups of this study enables a more accurate representation of the pressure and water supply aspects of downhole conditions.
- The contact area between cement paste and formation water body can largely affect the pore pressure variation. The larger the contact area, the slower cement pore pressure drops.
- The drastic decline of permeability majorly contributes to the rapid decrease of the cement pore pressure during the Initial Set and Hardening Stage
- The Initial Set and Hardening Stages are the key periods that have the most important influence on the development of cement state of stress. Cement mechanical behaviors during these two stages need to be carefully examined.

Since the measurement approach presented is novel and due to the limitations of the experimental conditions (i.e. ignorance of thermal factor), insufficiencies definitely exist and multiple improvements can be made. Further work majorly includes three categories:

(1) Improvement based on the current set-ups. Curing time should be extended until the cement pore pressure decrease slows down. Sensitivity analyses need to be performed for factors, which affect pore pressure evolution, such as water cement ratio and confining pressure.

(2) Additions to the current experimental set-ups to better characterize the downhole conditions. The inclusion of heating elements and the insulating material is planned to be incorporated into the current set-up. The mold for cement curing can also be replaced by a rock ring which allows for water entering the cement through the permeable rock matrix to replicate differences between formation/cement pore pressure and fluid flow through porous media.

(3) The combination with numerical approaches to assist field operations will improve estimation of wellbore integrity issues, reducing long term operational costs, and improving the longevity of well design. This will include mechanical property determination, and shrinkage characterization as inputs for numerical modeling. The study works to improve estimation of the initial state of stress of hardened cement, for modeling cement failure to assess the occurrence of wellbore integrity issues during subsequent wellbore operations during the life cycle of the well (i.e. loading cycles for hydraulic fracturing, pressure variation for the leak-off test, thermal cycling for injection).

Acknowledgments

The authors would like to acknowledge the Chevron ETC for financing the work. We are also grateful for the CalPortland Company for providing the cement for tests, Dr. Abdulmohsin Imqam for sharing the lab space, and Jeff Heniff for helping us with performing the experiment.

Nomenclature

API = *American Petroleum Institute*
WOC = *Wait on Cement*
w/c = *water cement ratio*

References

1. Appleby S, Wilson A. Permeability and suction in setting cement. Chemical Engineering Science. 1996 Jan 1;51(2):251-67.
2. Backe, K. R., Lile, O. B., Lyomov, S. K., Elvebakk, H., & Skalle, P. (1999, September 1). Characterizing Curing-Cement Slurries by Permeability, Tensile Strength, and Shrinkage. Society of Petroleum Engineers. doi:10.2118/57712-PA
3. Bois AP, Garnier A, Rodot F, Sain-Marc J, Aimard N. How to prevent loss of zonal isolation through a comprehensive analysis of microannulus formation. SPE Drilling & Completion. 2011 Mar 1;26(01):13-31.
4. Bois AP, Garnier A, Galdiolo G, Laudet JB. Use of a mechanistic model to forecast cement-sheath integrity. SPE Drilling & Completion. 2012 Jun 1;27(02):303-14.
5. Bourissai, M., Meftah, F., Brusselle-Dupend, N., Lécolier, É. and Bonnet, G., 2013. Evolution of the elastic properties of an oilwell cement paste at very early age under downhole conditions: Characterization and modelling. *Oil & Gas Science and Technology–Revue d'IFP Energies nouvelles*, *68*(3), pp.595-612.
6. Justnes H, Skalle P, Sveen J, Øye BA. Porosity of oil well cement slurries during setting. Advances in Cement Research. 1995 Jan;7(25):5-12.
7. Lavrov A, Torsæter M. Physics and mechanics of primary well cementing. Springer International Publishing; 2016 Aug 25.
8. Nelson EB, Guillot D. Well Cementing, 773. Sugar Land, Texas: Schlumberger. 2006.
9. Nygaard R, Salehi S, Weideman B, Lavoie RG. Effect of dynamic loading on wellbore leakage for the wabamun area CO2-sequestration project. Journal of Canadian Petroleum Technology. 2014 Jan 1;53(01):69-82.
10. Pang X, Jimenez WC, Iverson BJ. Hydration kinetics modeling of the effect of curing temperature and pressure on the heat evolution of oil well cement. Cement and Concrete Research. 2013 Dec 1;54:69-76.
11. Ravi K, Bosma M, Gastebled O. Improve the economics of oil and gas wells by reducing the risk of cement failure. InIADC/SPE Drilling Conference 2002 Jan 1. Society of Petroleum Engineers.
12. Reddy BR, Xu Y, Ravi K, Gray DW, Pattillo P. Cement Shrinkage measurement in oilwell cementing-A comparative study of laboratory methods and procedures. InRocky Mountain Oil & Gas Technology Symposium 2007 Jan 1. Society of Petroleum Engineers.
13. Specification AP. 10A, Specification for cements and materials for well cementing. American Petroleum Institute Publishing Services. Washington DC. 2002.
14. Wang HF. Theory of linear poroelasticity with applications to geomechanics and hydrogeology. Princeton University Press; 2017 Feb 15.
15. Zhang J, Weissinger EA, Peethamparan S, Scherer GW. Early hydration and setting of oil well cement. Cement and Concrete research. 2010 Jul 1;40(7):1023-33.
16. Zhang W, Eckert A, Liu X. Numerical simulation of micro-annuli generation by thermal cycling. In51st US Rock Mechanics/Geomechanics Symposium 2017 Aug 28. American Rock Mechanics Association.